

We are IntechOpen, the world's leading publisher of Open Access books Built by scientists, for scientists

6,900

Open access books available

185,000

International authors and editors

200M

Downloads

Our authors are among the

154

Countries delivered to

TOP 1%

most cited scientists

12.2%

Contributors from top 500 universities



WEB OF SCIENCE™

Selection of our books indexed in the Book Citation Index
in Web of Science™ Core Collection (BKCI)

Interested in publishing with us?
Contact book.department@intechopen.com

Numbers displayed above are based on latest data collected.
For more information visit www.intechopen.com



Embedded Control of the DC Drive System for Education

Marian Gaiceanu

Additional information is available at the end of the chapter

<http://dx.doi.org/10.5772/67461>

Abstract

Taking into account the spread use of the DC motor in robotics, the main objective of the chapter is to promote the knowledge regarding the development of the DC drive system, in didactical manner. Basically, for one motor control the cascaded loop DC drive system is used. Numerical implementation of the DC drive system based on Z-transform discrete method is provided. The electrical drive supposes both control types: the torque and speed. The feedback signals of the control loops are provided by using incremental encoder and of an original load torque estimator. Based on the DC motor dynamics, the appropriate parameters of the speed and torque controllers are provided automatically. On line parameters estimation of the DC motor can assure the performances of the DC drive controllers. The symmetrical and modulus optimum criteria are used. In order to prove the feasibility of the proposed solution, the entire Matlab script of the cascade control of the DC drive is provided. The strategy of the cascaded loop control at constant flux is divided into dynamic regime and into steady state regime. The chapter strategy follows two directions: the first, knowledge developments, the second, the applicative research through the real time implementation.

Keywords: Arduino, Matlab®, Simulink, H-bridge, DC motor, speed control, torque control, load torque estimator, discrete control system synthesis, Z-transform

1. Introduction

The chapter is addressed to researchers, students, and the users of industrial power converters and electric drives or mechatronics. The chapter contains the mandatory theoretical aspects and methods in order to develop successful DC drive system, being the most used in mechatronics applications. Upon implementing the proposed chapter applications, the readers will have the capability to develop own electric drive system, to bring the idea in practice very fast, and for better understanding of using the drive systems being open to add own contributions in

the mechatronics field. The chapter contains the basic concepts and techniques to design, simulate, and implement an electric drive system through a well-structured technical guide. By completing this chapter, the researchers will be familiarized with applying the concepts and techniques to manage adequately an electric drive system, widely found in industry and in mechatronics projects. The chapter strategy follows two directions: first, the theoretical approach (a practical discretization method is provided), and the second, the applicative research (numerical simulations and real-time implementations are provided). The chapter contains a high level of the cross-disciplinarily: electric machines, power electronics converters, Matlab/Simulink, real-time implementation, electrotechnics, measurements, and advanced control techniques.

In Section 2, an overview of the adjustable DC drives is given with the purpose to point out the development trend in the technology. In the next section, the dynamical equations of the DC drive system are provided. Section 4 contains the design of the rotor current and speed controllers. The load torque estimator is described in Section 5. Section 6 comprises the energetically model of the DC drive. Based on the on-line parameters identification procedure [1] the energy balance of the DC drive is performed and the appropriate energetic model is deduced in the Section 6 [2]. The optimal control based on linear quadratic controller is designed in the Section 7. The numerical approach by using Z-transform is provided in Section 8, and the simulation results are provided in Section 9. The real-time implementation of the speed control is included in Section 10. The conclusions of the chapter are placed in Section 11. The entire Matlab script is provided.

2. Overview of the DC drives

The DC machine can be controlled by using power converters. At low speed, the DC drives are very often used. There are two mainly control techniques: armature voltage control (constant torque region) and field current control (constant power region). The armature voltage control is obtained by maintaining constant field current and the field current control by maintaining the constant armature voltage [3].

3. The mathematical model of the DC drive system

Under certain hypotheses, the mathematical model of the DC machine could be obtained in state space form.

Supposing a constant value of the DC motor parameters, the DC machine has the compensated winding, the magnetic flux maintained at the constant value, the state space mathematical model of the DC machine becomes as follows [2]:

$$\begin{bmatrix} \frac{dn(t)}{dt} \\ \frac{di_A(t)}{dt} \end{bmatrix} = \begin{bmatrix} -\frac{F_v}{J} & \frac{C_m}{cJ} \\ -\frac{C_e}{T_A R_A} & -\frac{1}{T_A} \end{bmatrix} \cdot \begin{bmatrix} n(t) \\ i_A(t) \end{bmatrix} + \begin{bmatrix} 0 \\ \frac{1}{T_A R_A} \end{bmatrix} u(t) + \begin{bmatrix} -\frac{1}{cJ} \\ 0 \end{bmatrix} T_L(t) \quad (1)$$

in which J is the reduced inertia moment to the electric motor shaft, T_A , the armature time constant, R_A , the armature resistance, and the specific constants

$$c_t = \frac{\pi}{30}, \quad C_m = k\phi, \quad C_e = c_t C_m, \quad (2)$$

in which k is the DC motor constant.

The state vector of the DC machine contains two states, $\mathbf{x}(t) = \begin{bmatrix} n(t) \\ i_A(t) \end{bmatrix}$, the control vector is only the rotor voltage $\mathbf{u}(t) = u_A(t)$, the perturbation vector is the load torque $\mathbf{w}(t) = T_L(t)$, and the output of the DC motor is the speed $\mathbf{y}(t) = n(t)$. Under these circumstances, the mathematical model of the DC motor becomes

$$\begin{aligned} \dot{\mathbf{x}}(t) &= \mathbf{A} \cdot \mathbf{x}(t) + \mathbf{B} \cdot \mathbf{u}(t) + \mathbf{G} \cdot \mathbf{w}(t) \\ \mathbf{y}(t) &= \mathbf{C} \cdot \mathbf{x}(t), \end{aligned} \quad (3)$$

Taking into consideration the above mentioned hypothesis, the mathematical model of the DC motor Eq. (1) is linear and invariant.

In order to obtain variable speed, there are two topologies of the power converters for DC motor applications: ac-dc and dc-dc. The mathematical model of the power converter, under certain conditions (continuous conduction, neglecting the voltage drop in conduction mode), represents an ideal power amplifier k_D [2].

4. The cascaded loop control of the DC drive system

The DC drive contains two control loops: the inner—the armature current loop and the outer—the speed loop, **Figure 1** [2]. Therefore, the control is in cascaded manner. The current feedback is delivered through an adequate current sensor and the speed feedback is obtained based on numerical derivative of the encoder signals. The desired speed is set as reference signal from a potentiometer. Due to the higher power necessity, the dc-dc four quadrants power converter is added. Therefore, by means of the DC voltage control of the DC machine, the torque and speed are adequately adjusted according to the references. The parameters of the current regulator are obtained by using the *modulus criterion*, and the parameters of the speed controller are delivered by using the *symmetrical optimum criterion* (Kessler version).

By taken into account the 10 (V) voltage unified system, the transfer function of the proportional-integral (PI) current controller is expressed as

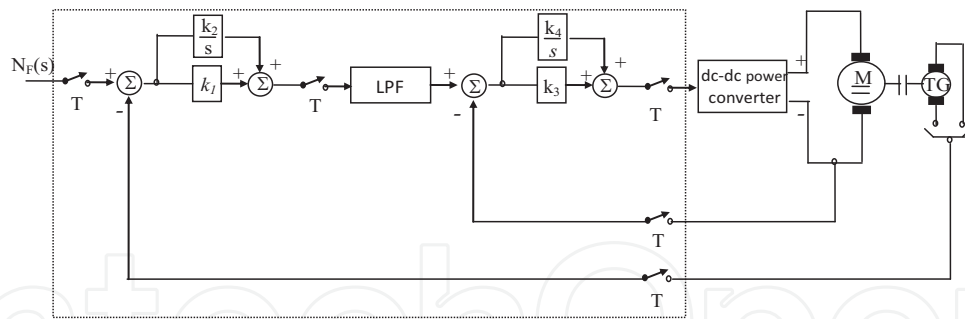


Figure 1. Block diagram of the digital DC speed cascaded control.

$$H_{RI}(s) = k_3 + \frac{k_4}{s} \tag{4}$$

with the following parameters [2]:

$$k_3 = \frac{T_A R_A^A}{2T_{\Sigma I} k_D k_I}, \quad k_4 = \frac{R_A}{2T_{\Sigma I} k_D k_I} \tag{5}$$

where:

- $k_D = \frac{U_N}{10}$, transfer function of the dc-dc power converter;
- $k_I = \frac{10}{I_{Amax}} \left[\frac{V}{A} \right]$, attenuation factor of the current transducer;
- $T_{\Sigma I} = T_I$ the sum of the parasitic time constant of the current loop is determined by the time constant of the current transducer.

The transfer function of the PI speed controller has the form:

$$H_{RT}(s) = k_1 + \frac{k_2}{s} \tag{6}$$

the parameters of the speed controller [2] being deducted from symmetrical optimum criterion:

$$k_1 = \frac{k_I C J}{2T_{\Sigma N} C_m k_T} \tag{7}$$

$$k_2 = \frac{k_I C J}{8T_{\Sigma N}^2 C_m k_T} \tag{8}$$

in which:

- $k_T = \frac{10}{n_N} \left[\frac{V}{rpm} \right]$, attenuation factor of the speed transducer;
- $T_{\Sigma N} = 2 \cdot T_{\Sigma I} + T_N$, the sum of the parasitic time constants of the speed loop, T_N being the time constant of the speed transducer.

5. Load torque estimator

In **Figure 2**, the operational model of the load torque estimator [4, 5] is shown. The calculus of the load torque estimator parameters is based on the imposed performances: desired pulsation ω_0^* , and the desired overshoot ξ^* , respectively:

$$\tau = \frac{2\xi^*}{\omega_0^*} \quad (9)$$

$$c = 2\xi^* \omega_0^* \quad (10)$$

IntechOpen

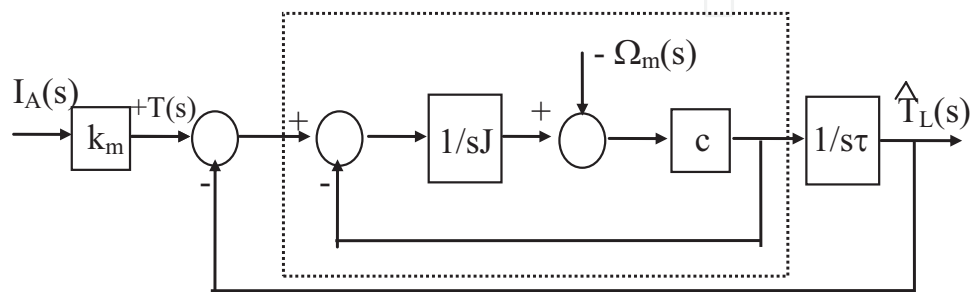


Figure 2. The second-order load torque estimator [2].

6. The energetically model of the DC drive

Based on the mathematical model of the DC machine Eq. (1), the energetic model has been deduced (**Figure 3**) [2], in which T_o is the mechanical friction torque, T_{Fv} —the viscous force equivalent torque, T_f —the Foucault currents losses equivalent torque, and T_H —the hysteresis losses equivalent torque.

By using the electrical and mechanical equations of the DC motor at the constant flux, the energetic components of the DC drive are obtained:

IntechOpen

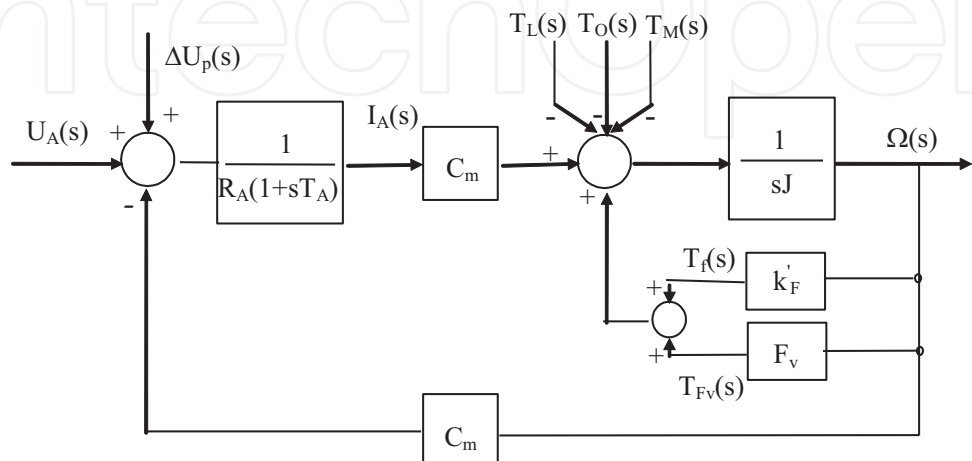


Figure 3. The energetic model of the DC machine.

$$u_A(t) = R_A \cdot i_A(t) + L_A \cdot \frac{di_A(t)}{dt} + e(t) + \Delta u_p(t) \quad (11)$$

$$T_e(t) = T_L(t) + F_v \cdot \Omega(t) + J \cdot \frac{d\Omega(t)}{dt}. \quad (12)$$

By multiplying Eq. (11) with $i_A(t)$ term, and Eq. (12) with $\Omega(t)$, the power balance of the DC drive can be obtained. In this way, the specific power components are obtained:

- The electrical power

$$P_1(t) = u_A(t) \cdot i_A(t) \quad (13)$$

- Different expressions of the electromagnetic power

$$P(t) = T_e(t) \cdot \Omega(t) = C_m i_A(t) \Omega(t) = e(t) i_A(t) \quad (14)$$

- The rotor copper power losses

$$P_{cu} = R_A \cdot i_A^2(t) \quad (15)$$

- The accumulated power in the rotor inductance

$$P_L = L_A i_A(t) \frac{di_A(t)}{dt} \quad (16)$$

- The brush power losses

$$P_p(t) = \Delta u_p(t) \cdot i_A(t) \quad (17)$$

- The mechanical power

$$P_u(t) = T_L(t) \cdot \Omega(t) \quad (18)$$

- The accumulated power in the rotational masses

$$P_j = J \Omega(t) \frac{d\Omega(t)}{dt} \quad (19)$$

- The viscous power losses

$$P_f(t) = T_f \cdot \Omega(t) \quad (20)$$

The magnetization frequency of the rotor ferromagnetic core is

$$f = \frac{p\Omega(t)}{2\pi}. \quad (21)$$

At the constant flux, the total core losses are

$$p_{Fe} = k_H \cdot f + k_F \cdot f^2 \quad (22)$$

or by

$$p_{Fe}(t) = k'_H \Omega(t) + k'_F \Omega^2(t). \quad (23)$$

Taking into consideration the deducted magnetic core losses Eq. (23), the corresponding equivalent torque is as follows

$$T_{Fe}(t) = \frac{P_{Fe}}{\Omega(t)} = k'_H + k'_F \cdot \Omega(t) \quad (24)$$

or denoted by:

$$T_{Fe}(t) = T_H(t) + T_F(t). \quad (25)$$

The mechanical losses are constant. Therefore, the corresponding torque is as follows:

$$T_0(t) = \frac{P_0}{\Omega(t)}. \quad (26)$$

By applying the Laplace transform to Eqs. (11) and (12), the electromechanical model of the DC motor at constant flux is obtained:

$$U_A(s) - E(s) - \Delta U_p(s) = R_A I_A(s) + sL_A I_A(s) \quad (27)$$

$$T(s) = T_L(s) + T_0(s) + T_H(s) + T_F(s) + T_f + sJ\Omega(s) \quad (28)$$

Based on Eqs. (27) and (28), the energetic operational model of the DC motor is obtained as in **Figure 3** [2].

6.1. Estimation of the DC drive losses components

By using zero-order hold, the numerical energies are calculated as a sum of the local areas:

$$\sum_{i=0}^N V_i T \quad (N \text{ the maximum sampling interval with constant sampling time } T).$$

The losses in the rotor windings at the k -th sampling time are as follows:

$$\Delta P_{Cu}(kT) = R_A \cdot I_A^2(kT), \quad (29)$$

and the total rotor copper energy over the control interval can be deducted as

$$\Delta W_{Cu} = \sum_{i=1}^N R_A \cdot I_A^2(iT) \cdot T. \quad (30)$$

In the same way, the following energies are calculated:

- The input energy of the DC motor

$$W_{P_1} = \sum_{i=1}^N U(iT) \cdot I_A(iT) \cdot T \quad (31)$$

- The accumulated energy in the rotor inductance

$$\Delta W_L = \sum_{i=1}^N L_A \cdot I_A(iT) \cdot [I_A(iT) - I_A((i-1)T)] \quad (32)$$

- The accumulated energy in the rotational mass

$$\Delta W_J = \sum_{i=1}^N J \cdot \Omega(iT) \cdot [\Omega(iT) - \Omega((i-1)T)] \quad (33)$$

The brush, the mechanical, and the core losses have been ignored.

By knowing the above mentioned energies, the output energy could be calculated:

$$W_{out} = W_{P_1} - \Delta W_{Cu} - \Delta W_L - \Delta W_J \quad (34)$$

By using the same methodology, the losses of the power converter and the transformer are obtained.

7. Linear quadratic control

The DC machine operates at maximum efficiency at rated operating point, therefore, in steady state. During transient regime, the copper losses component is the higher loss in the DC machine. In order to reduce the power losses in DC drive, the optimal control block diagram is proposed. The proposed solution combines the advantages of the conventional cascaded control (PI) and optimal control [6, 7]. The designed software switch goes in position 1 when the speed error is zero, otherwise goes in position 2 (**Figure 4**).

7.1. Problem formulation

The problem statement of the optimal control supposes a design of the performance index (functional cost). By minimizing the functional cost, the optimal control solution is obtained without any constraints. The optimal control limits are controlled by introducing the weighting matrices [6, 7]. The objectives of the optimal control include the objectives of the conventional drive system (regulation, stability assurance, and robustness to perturbations) and the energy reduction.

The gate drive control is denoted by GDC, the voltage control by u_c (Figure 4), the load torque estimator by TL estimator block, the tacho generator by TG, the imposed speed reference and the imposed firing angles. The switch is toggled between position 1 (for conventional control) and fixed position 2 (for optimal control). The conventional control is activated during the steady-state regimes, and the optimal control is activated during transients (starting, stopping, and reversing regimes).

In order to control the DC motor in an optimal manner (Figure 5), the adopting functional cost is with infinite time horizon:

$$J = \frac{1}{2} \int_0^{\infty} [x^T(t)Qx(t) + u^T(t)Ru(t)]dt. \quad (35)$$

By minimizing the adopted performance function, the optimal control is delivered:

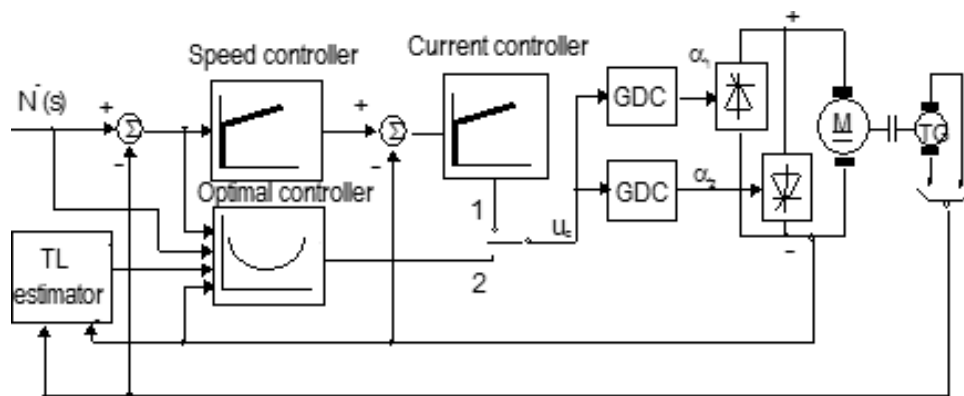


Figure 4. Optimal control system of the DC motor at constant flux.

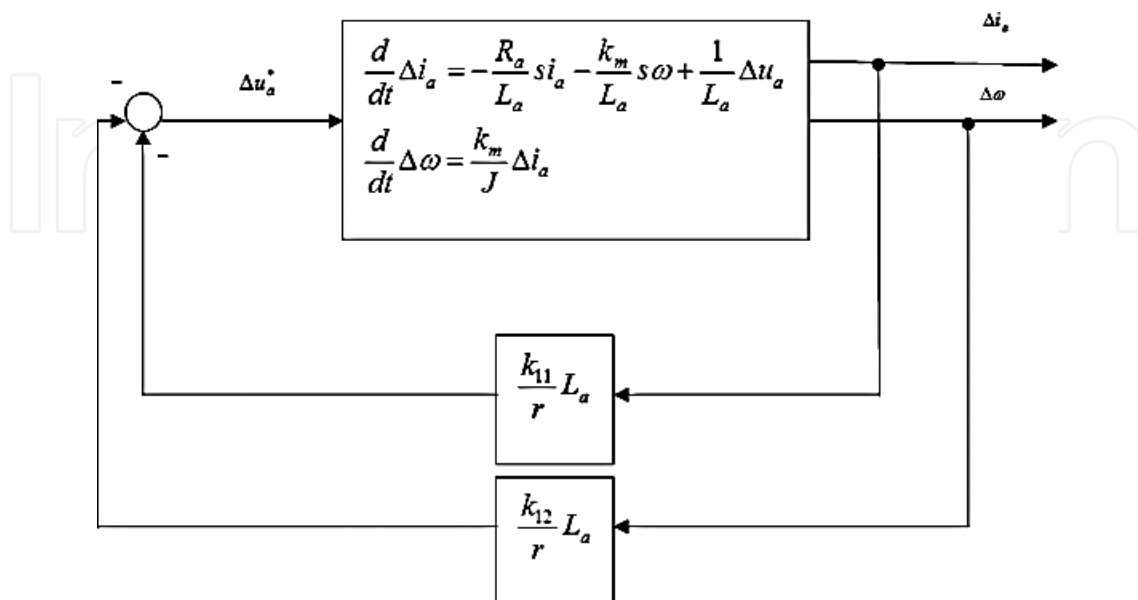


Figure 5. The optimal DC drive system.

$$u^*(t) = -\mathbf{R}^{-1}\mathbf{B}^T\mathbf{K}\mathbf{x}(t), \tag{36}$$

in which the symmetrical gain matrix \mathbf{K} :

$$\mathbf{K} = \begin{bmatrix} k_{11} & k_{12} \\ k_{21} & k_{22} \end{bmatrix} > 0, \tag{37}$$

is the solution of the algebraic Riccati equation (ARE):

$$\mathbf{K}\mathbf{A} + \mathbf{A}^T\mathbf{K} - \mathbf{K}\mathbf{B}\mathbf{R}^{-1}\mathbf{B}^T\mathbf{K} + \mathbf{Q} = \mathbf{0}. \tag{38}$$

8. Numerical implementation of the DC drive system

The continuous signals are converted into digital format by using sampling and hold stages. The reversibility takes place through the digital-to-analog converters (DACs), that is, the digital signals are converted into continuous ones.

The properties of the zero-order hold are to maintain the captured signal at the constant value over the entire sampling period. Therefore, the obtained transfer function is

$$H_{zoh}(s) = \frac{1 - e^{-sT}}{s}. \tag{39}$$

8.1. Mathematical model of the digital current control loop

In **Figure 6**, the block diagram of the numerical model of the current loop is shown [2].

The switch symbol from **Figure 6** represents the sampling and hold process, T being the sampling time.

The transfer between the “ s ” plane and “ Z ” one is made by using the Z -transform. By using the transfer function of the zero-order hold, the discrete transfer function could be obtained according to

$$H_{FI}(z^{-1}) = Z[H_{EOZ}(s) \cdot H_{FI}(s)] \tag{40}$$

or in the other form

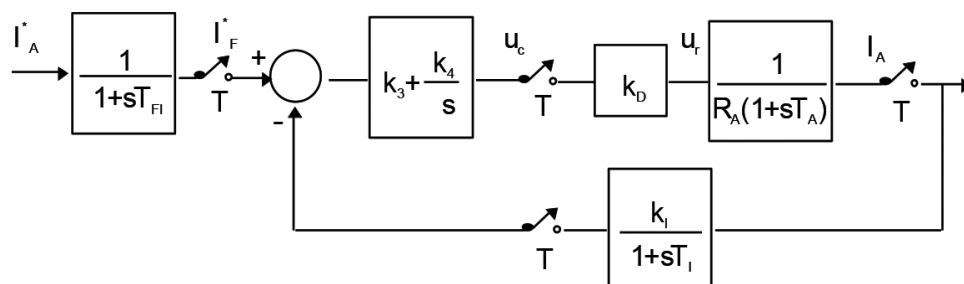


Figure 6. The armature current control loop.

$$H_{FI}(z^{-1}) = Z \left[\frac{1 - e^{-sT}}{s} \cdot \frac{1}{1 + sT_{FI}} \right]. \quad (41)$$

Taking into account that $z = e^{sT}$, the discrete transfer function Eq. (41) becomes

$$H_{FI}(z^{-1}) = \frac{1 - z^{-1}}{T_{FI}} \cdot Z \left[\frac{1}{s \left(s + \frac{1}{T_{FI}} \right)} \right]. \quad (42)$$

Taking into account the residuum theorem of the simple poles, the Z-transform can be calculated as

$$H_{FI}(z^{-1}) = \frac{1 - z^{-1}}{T_{FI}} \cdot \left[\frac{1}{\frac{1}{T_{FI}}} \cdot \frac{1}{1 - z^{-1} \cdot e^{T \cdot 0}} + \frac{1}{-\frac{1}{T_{FI}}} \cdot \frac{1}{1 - z^{-1} \cdot e^{-\frac{T}{T_{FI}}}} \right]. \quad (43)$$

By the other side:

$$H_{FI}(z^{-1}) = \frac{I_{FI}^*(z^{-1})}{I_A^*(z^{-1})}. \quad (44)$$

By taking into consideration Eqs. (43) and (44), the following recurrent relation is obtained

$$I_{FI}^*(k) = I_{FI}^*(k-1) \cdot e^{-\frac{T}{T_{FI}}} + I_A^*(k-1) \cdot \left(1 - e^{-\frac{T}{T_{FI}}} \right). \quad (45)$$

By starting from the current transducer transfer function

$$\frac{I_R(s)}{I_A(s)} = \frac{k_I}{1 + sT_I} \quad (46)$$

a similar recurrent equation for the current feedback is obtained:

$$I_R(k) = I_R(k-1) \cdot e^{-\frac{T}{T_I}} + I_A(k-1) \cdot \left(1 - e^{-\frac{T}{T_I}} \right) \cdot k_I. \quad (47)$$

The discrete implementation of the current controller

$$H_{RI}(s) = k_2 + \frac{k_4}{s}, \quad (48)$$

is made by using in the similar manner as for the current filter and using the linearity propriety of the Z-transform

$$H_{RI}(z^{-1}) = k_3(1 - z^{-1})Z \left[\frac{1}{s} \right] + k_4(1 - z^{-1})Z \left[\frac{1}{s^2} \right]. \quad (49)$$

On the other hand

$$H_{RI}(z^{-1}) = \frac{U_C(z^{-1})}{I_{FI}^*(z^{-1}) - I_R(z^{-1})}. \quad (50)$$

Taking into account the Z-transform table, and using Eqs. (49) and (50), the digital implementation of the current regulator is

$$U_c(k) = U_c(k - 1) + k_3 \cdot [I_{FI}^*(k) - I_R(k)] + (k_4T - k_3)[I_{FI}^*(k - 1) - I_R(k - 1)]. \quad (51)$$

Taking into consideration the dc-dc power converter ideal amplifier model, the rotor voltage is obtained:

$$u_A(k) = k_D u_c(k). \quad (52)$$

By taken into consideration one of the following equations, the output signal of the rotor current loop is obtained:

- By neglecting the electromotive voltage

$$I_A(k) = I_A(k - 1) \cdot e^{-\frac{T}{T_A}} + u_A(k - 1) \cdot \left(1 - e^{-\frac{T}{T_A}}\right) \cdot \frac{1}{R_A} \quad (53)$$

- By considering the electromotive voltage

$$I_A(k) = I_A(k - 1) \cdot e^{-\frac{T}{T_A}} + [u_A(k - 1) - C_e N(k - 1)] \cdot \left(1 - e^{-\frac{T}{T_A}}\right) \cdot \frac{1}{R_A}. \quad (54)$$

8.2. Mathematical model of the digital speed control loop

In **Figure 7**, the block diagram of the digital speed control loop is shown, in which the equivalent closed loop transfer function of the armature current control is replaced by current loop block.

Taking into consideration the block diagram shown in **Figure 7**, in the similar manner, the digital implementation of the speed loop is obtained.

Therefore, the imposed filtered speed is

$$N_{FT}^*(k) = N_{FT}^*(k - 1) \cdot e^{-\frac{T}{T_{FT}}} + N^*(k - 1) \cdot \left(1 - e^{-\frac{T}{T_{FT}}}\right). \quad (55)$$

The digital equation of the recurrent feedback speed is

$$N_R(k) = N_R(k - 1) \cdot e^{-\frac{T}{T_r}} + N^*(k - 1) \cdot \left(1 - e^{-\frac{T}{T_r}}\right) k_T. \quad (56)$$

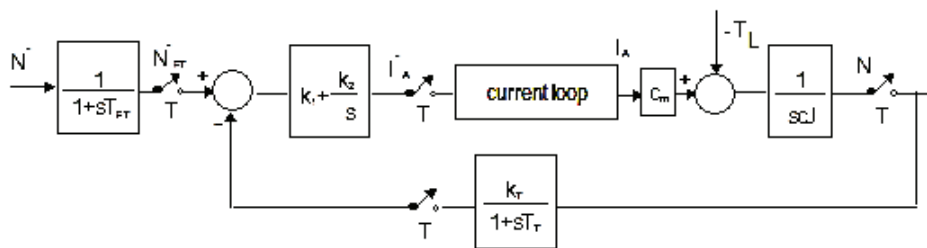


Figure 7. The speed control loop.

The speed controller for numerical implementation is as:

$$I_A^*(k) = I_A^*(k-1) + k_1 \cdot [N_{FT}^*(k) - N_R(k)] + (k_2 T - k_1)[N_{FT}^*(k-1) - N_R(k-1)], \quad (57)$$

with the obtained numerical signal of the speed feedback

$$N(k) = N(k-1) + \frac{T}{cJ} \cdot [C_m I_A(k-1) - T_L(k-1)]. \quad (58)$$

By organizing the numerical equations in the specified order Eqs. (55)–(57), (45), (47), (51)–(53), (58), the digital representation of the DC drive system is obtained.

9. Numerical simulation results

Taking into consideration the following DC motor of 12 W, 12 V/1 A, 90 r.p.m. at rated load torque of 1.37 Nm, the cascaded control loops are implemented in Matlab by using the deduced numerical equations. The following numerical results have been obtained.

In **Figure 8** (left side), the dynamic mechanical characteristic for a starting under different load torque variation (**Figure 8**, right side) is shown. At the same time, in **Figure 9**, the implemented load torque estimator result is presented.

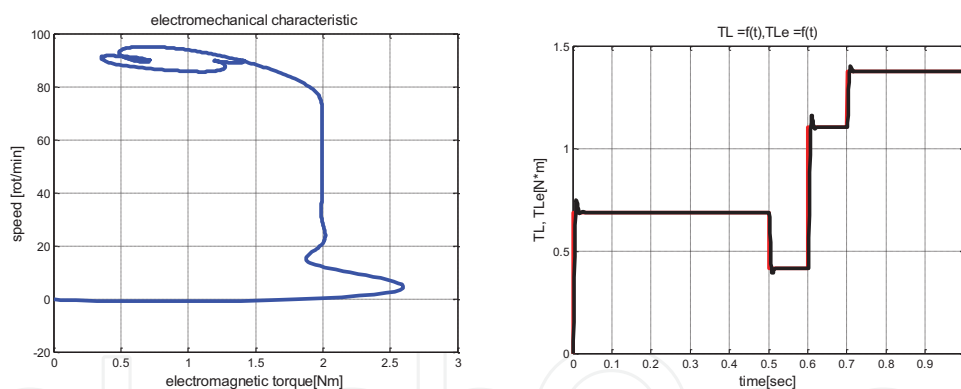


Figure 8. Mechanical characteristic of the DC motor (left side). Real (step signal) and the estimated load torque (delayed signal).

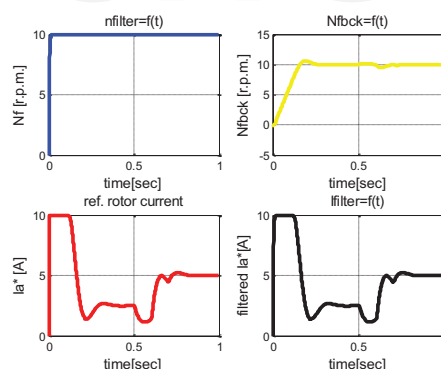


Figure 9. The control signals of the DC drive.

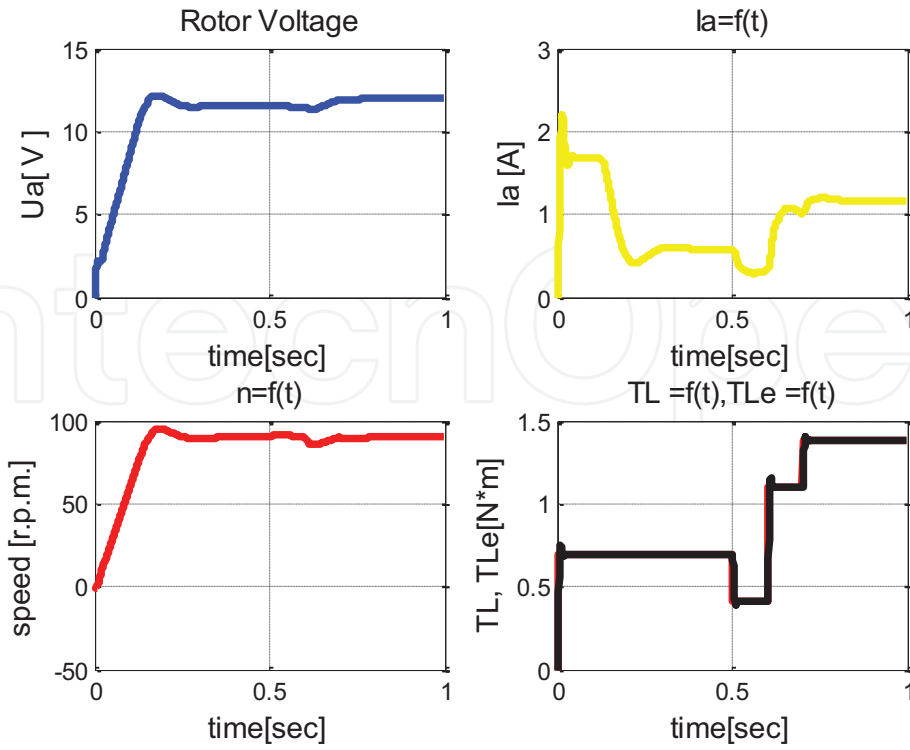


Figure 10. The power signals of the DC drive.

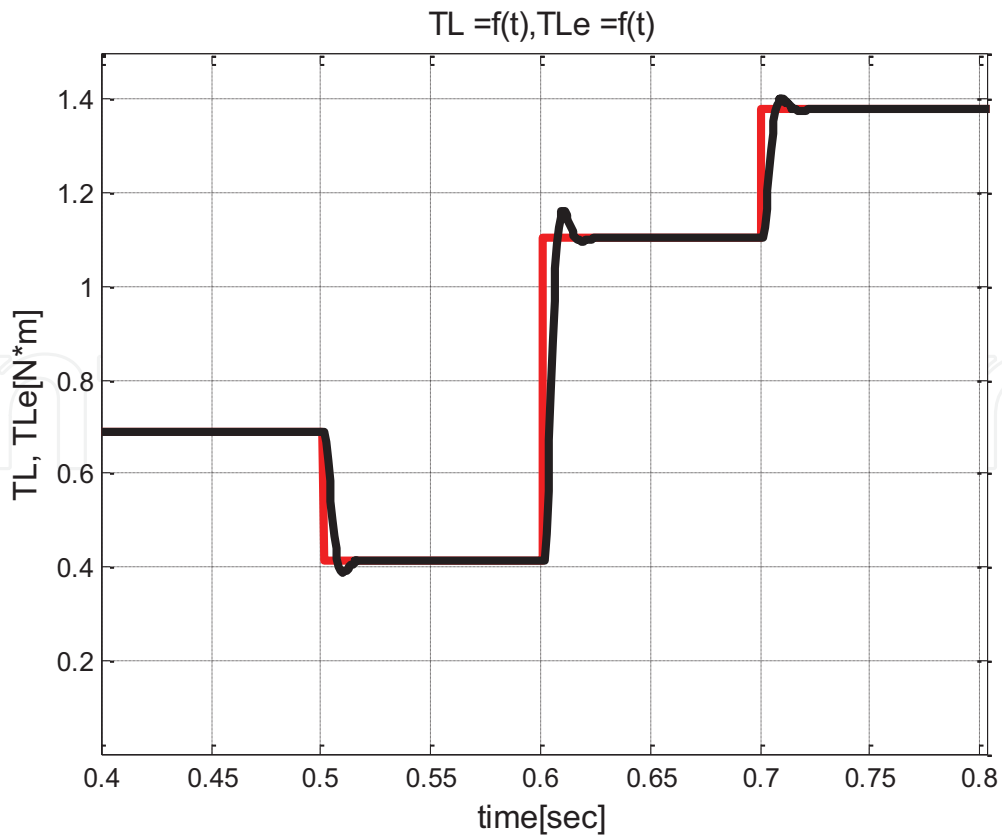


Figure 11. The performances of the second-order load torque estimator.

Based on the above mentioned digital implementation and taking into consideration that the DC drive is formed by two parts, control and power, the following simulation results are obtained. Therefore, on the control side, there are only analog voltages ([0–10] V unified system) (**Figure 9**). On the power side, the real signals are shown (**Figure 10**). In **Figure 9**, the following DC drive signals are shown: the filtered speed reference (n_{filter}), the feedback speed (N_{fbck}), the output of the speed controller (i.e., the reference of the rotor current, *ref. rotor current*), and the filtered rotor current reference (I_{filter}).

On power side, the real values of the DC drive signals are presented: the rotor voltage (U_a), the rotor current (I_a), the controlled feedback speed as the output signal of the DC drive (n), and the load torque signals (the real, T_L and the estimated, T_{Le}). The more accurate estimator performances are presented on the [0.4–0.8]s time interval, in **Figure 11**.

10. Real-time speed control

Based on the Arduino platform, the conventional control of the DC drive system is implemented in real time (**Figure 12**). It consists of the cascaded control, on-line estimation of the DC motor parameters (**Figure 13**) based on the recursive least squares method [1], and real-time estimation of the load torque (**Figure 14**) [2]. The speed feedback is assured by using an incremental encoder [8]. In order to improve the speed response of the DC drive system, a feedforward additional voltage component has been introduced, as in **Figure 15** [9]. In **Figures 16–18**, the build s-function and the associated Simulink blocks for speed and position calculus from the encoder signals are shown.

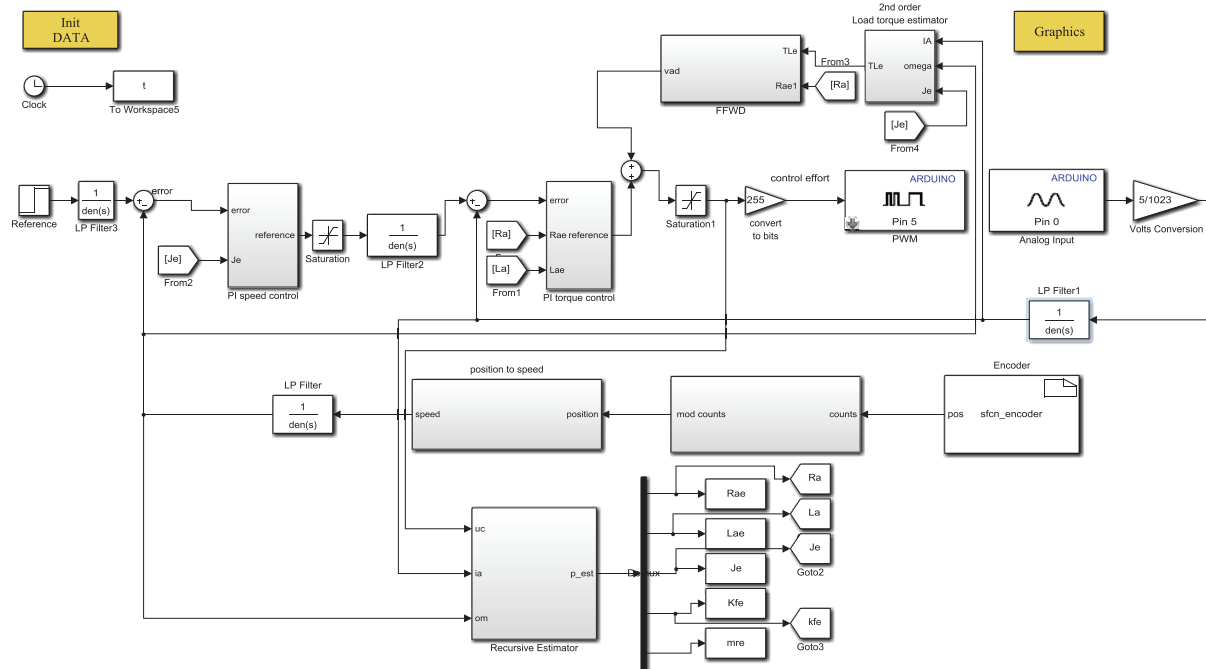


Figure 12. The embedded DC drive cascaded control.

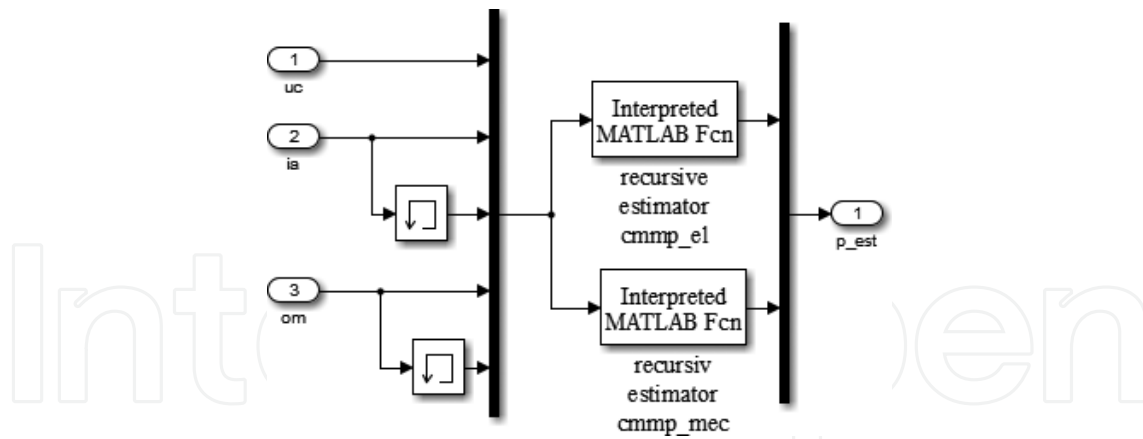


Figure 13. The on-line estimator of the DC motor.

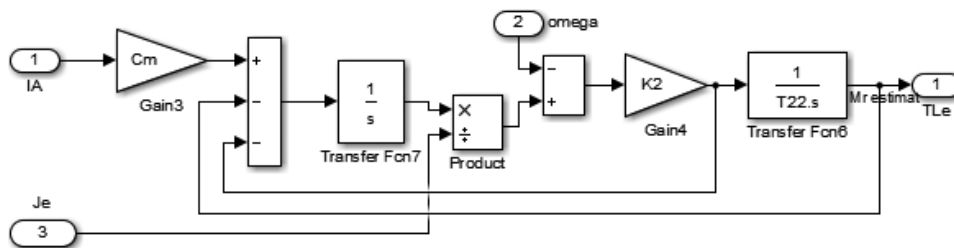


Figure 14. The second-order load torque estimator.

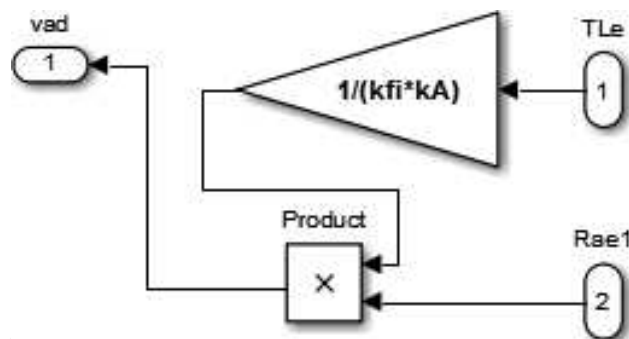


Figure 15. The feedforward control voltage component.

The appropriate Matlab functions [1] from Figure 13 are delivered as follows:

```
function tetael=ctmp_el(in)
global tetael_an Pel_an lambda_el Kfi T
y=in(1)-Kfi*in(4);
fi=[ in(2); (in(2)-in(3))/T];
L=(Pel_an*fi)/(lambda_el+fi'*Pel_an*fi);
```

```
tetael=tetael_an+L*(y-fi'*tetael_an);
Pel=(Pel_an-(Pel_an*fi*fi'*Pel_an)/(lambda_el+fi'*Pel_an*fi))/
lambda_el;
tetael_an=tetael;
Pel_an=Pel;

function tetamec=cmp_mec(in)
global tetamec_an Pmec_an lambda_mec alphas denumm Pm Kfi T
y=Kfi*in(2);
fi=[(in(4)-in(5))/T;1;in(4)];
denumm=(lambda_mec+fi'*Pmec_an*fi);
L=(Pmec_an*fi)/denumm;
alphas=(y-fi'*tetamec_an);
tetamec=tetamec_an+L*alphas;
Pm=L*fi'*Pmec_an;
Pmec=(Pmec_an-Pm)/lambda_mec;
tetamec_an=tetamec;
Pmec_an=Pmec;
```

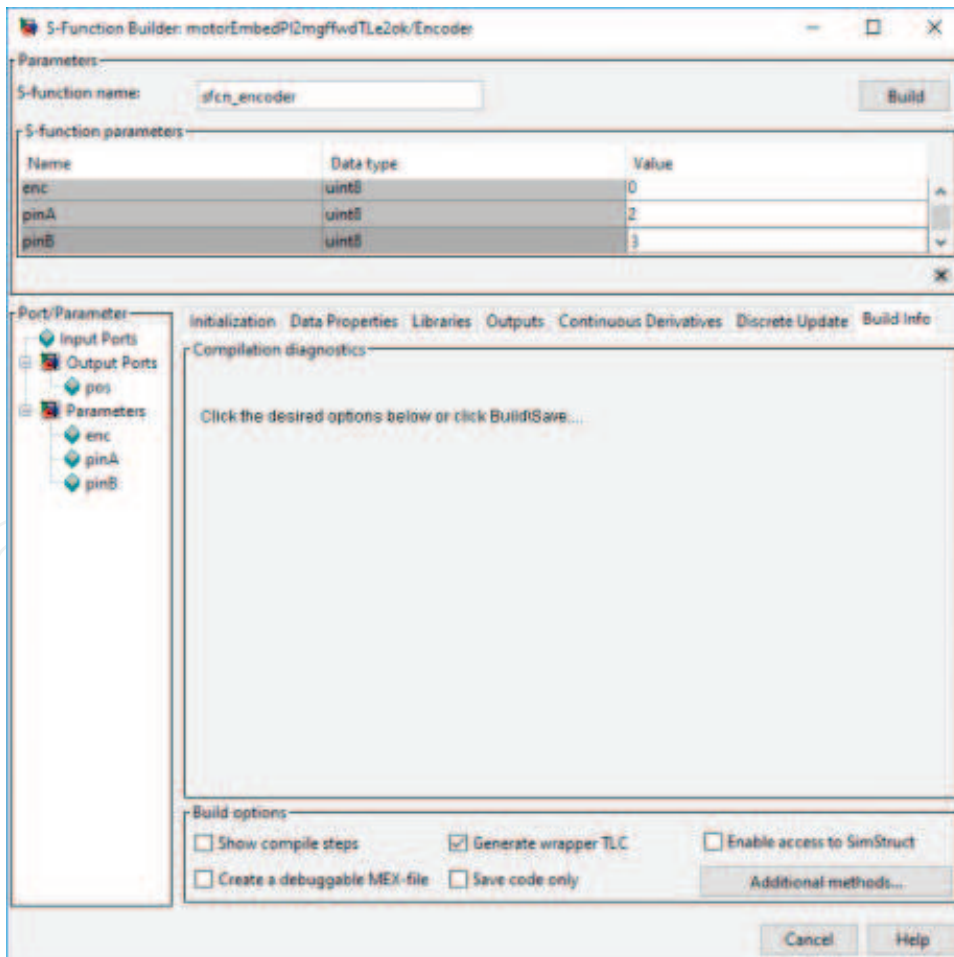


Figure 16. The s-function block of the encoder [8].

By applying the numerical derivative of the position adapted to gear ratio the real speed value is obtained (Figure 19).

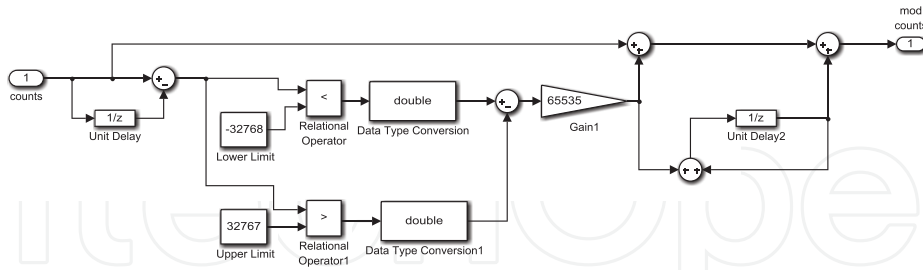


Figure 17. The calculus of the DC rotor position [8].

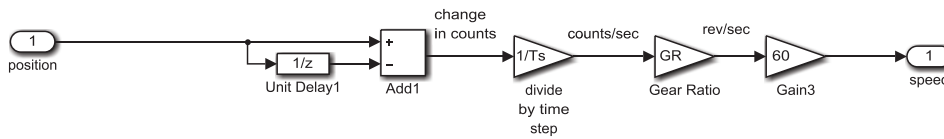


Figure 18. The numerical derivation of the position [8].

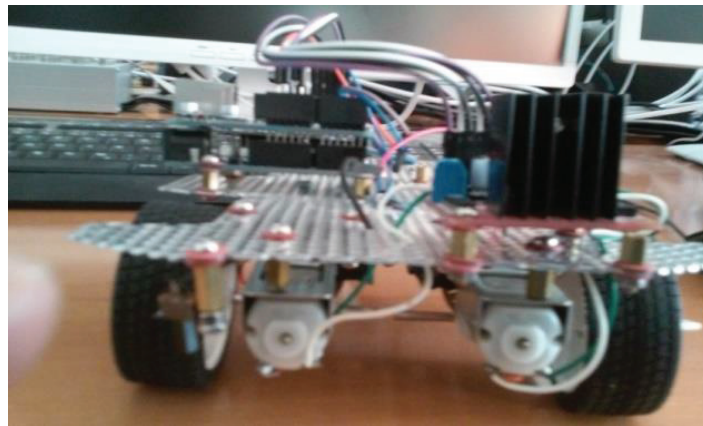


Figure 19. The DC drive platform.

11. Conclusions

This chapter is designed in the didactical manner that allows students and researchers to implement autonomously the mechatronic projects based on the DC drive. Starting from the nameplate data of the DC motor, the provided Matlab software has the ability to calculate the DC motor parameters, the parameters of the current and speed controllers, and includes the numerical implementation of the DC motor cascaded control, energy balance and of the load torque estimator. The price of the proposed DC drive is down due to the fact that the load torque is very expensive and it is replaced by the load torque estimator. By using the Z-transform, the procedure of numerical control is implemented. The implementation of the digital filters and controllers are also provided. Numerical simulations confirm the accuracy of the

proposed DC drive discretization method. Moreover, the real-time control based to Arduino platform has been performed. In order to increase the DC drive performances, the on-line estimator of the DC motor parameters is provided, and the feedforward control voltage component has been added.

Acknowledgements

This work was supported by a grant of the Romanian National Authority for Scientific Research, CNDI-UEFISCDI, project number PN-II-PT-PCCA-2011-3.2-1680.

Appendix

```
% CONVENTIONAL AUTOMATION OF THE DIRECT CURRENT MOTOR
clear;clf;
%
%          DC DRIVE SYSTEM
% Nameplate Data
%   -Rated Power
%     Pn=12      %W
%   -Rated Voltage
%     Un=12      %V
%   -Rated Speed
%     nn=90      %rot/min
%   -moment of inertia
%     Jt=0.02    %kgm^2
%     J=Jt;
%   -Rated efficiency
%     etan=0.86 %
% Main data calculus
%   -Electrical Power (input)
%     P1=Pn/etan %W
%   -Rated current
%     Ian=P1/Un  %A
%   -DC motor losses
%     deltap=P1-Pn %W
%   -Rated winding losses
%     pcun=deltap/2 %W
%   -Rotor resistance
%     Ra=pcun/(Ian^2) %ohmi
%   -Electromagnetic Power
%     P=Pn+deltap/2 %W
%   -Electromagnetic torque
%     Mn=30*P/pi/nn %Nm
%   -Mechanical constant
```

```

    kfi=Mn/Ian
    Cm=kfi
% -Electrical constant
    kefi=pi*kfi/30
    Ce=kefi
% -Electromotive voltage
    E=Ce*nn %V
% -Rotor resistance value check Ra
    Ra=(Un-E)/Ian %ohmi
% -volant moment
    g=9.81; %gravit. acc.
    GD2=4*g*Jt %m^2
% -Maximum torque
    Mmax=2*Mn %Nm
% -Maximum rotor current
    Iamax=Mmax/Cm %A
% -Electrical constant (from identification procedure) Ta
    Ta=7/(10^3) %sec
% -Rotor inductance
    La=Ta*Ra %H
% -Load torque
    Mr=1*Mn; %Nm
    k=pi/30;
%%%%%%%%%%%%%%%%%%%%%%%%%%%%%%%%%%%%%%%%%%%%%%%%%%%%%%%%%%%%%%%%%%%%%%%%
% Current loop- tuning of the controller parameters
% (modulus criterion - KESSLER variant)
%%%%%%%%%%%%%%%%%%%%%%%%%%%%%%%%%%%%%%%%%%%%%%%%%%%%%%%%%%%%%%%%%%%%%%%%
%current transducer
%%%%%%%%%%%%%%%%%%%%%%%%%%%%%%%%%%%%%%%%%%%%%%%%%%%%%%%%%%%%%%%%%%%%%%%%
% -for DC motor
    ka=1/Ra % (1/ohmi)
% -attenuation factor of the current transducer
    ki=10/Iamax % (V/A)
% -Current transducer time constant
    Ti=0.003 %sec
%%%%%%%%%%%%%%%%%%%%%%%%%%%%%%%%%%%%%%%%%%%%%%%%%%%%%%%%%%%%%%%%%%%%%%%%
%DC-DC Power Converter
%%%%%%%%%%%%%%%%%%%%%%%%%%%%%%%%%%%%%%%%%%%%%%%%%%%%%%%%%%%%%%%%%%%%%%%%
% -gain factor
    kd=Un/10
%%%%%%%%%%%%%%%%%%%%%%%%%%%%%%%%%%%%%%%%%%%%%%%%%%%%%%%%%%%%%%%%%%%%%%%%
% PI Current Controller
%%%%%%%%%%%%%%%%%%%%%%%%%%%%%%%%%%%%%%%%%%%%%%%%%%%%%%%%%%%%%%%%%%%%%%%%
% -sum of the parasitic constant of the current loop

```

```

    Tsi=Ti    %sec
%   -Proportional coefficient
    tau1=Ta    %sec
%   -gain factor
    k1=1/(2*Tsi*kd*ka*ki)
%   -Time constant of the current filter
    Tf1=Ti    %sec
%%%%%%%%%%%%%%%%%%%%%%%%%%%%%%%%%%%%%%%%%%%%%%%%%%%%%%%%%%%%%%%%%%%%%%%%
%   Speed loop- tuning of the controller parameters
%   (symmetrical criterion - KESSLER variant)
%%%%%%%%%%%%%%%%%%%%%%%%%%%%%%%%%%%%%%%%%%%%%%%%%%%%%%%%%%%%%%%%%%%%%%%%
%speed transducer
%%%%%%%%%%%%%%%%%%%%%%%%%%%%%%%%%%%%%%%%%%%%%%%%%%%%%%%%%%%%%%%%%%%%%%%%
%   -attenuation factor of the speed transducer
    kt=10/nn    % (V/r.p.m.)
%   -Time constant
    Tt=Ti    %sec
%   -gain factor of the mechanical inertia (1/s* Jt)
    kj=375/GD2;
%   PARAMETERS OF THE PI SPEED CONTROLLER
%   -sum of the parasitic constant of the speed loop
    Tst=2*Tsi+Tt    %sec
%   -Proportional coefficient
    tau2=4*Tst    %sec
%   -gain factor
    k2=ki/(kj*kt*Cm*8*(Tst^2))
%   -Speed time constant
    Tf2=Tt

%   NUMERICAL SIMULATION OF THE DC DRIVE SYSTEM
%   - sampling time
    T=Ta/10;    %sec
%   -initial conditions
%   a) current loop
    Ir=0;    %A    %output signal of the current transducer
    If=0;    %A    %output signal of the current filter Ii
    U=0;    %V    % DC-DC voltage
    Ia=0;    %A    % rotor current
%   b) speed loop
    Nf=0;    %r.p.m.    %output signal of the speed filter Ni
    Nr=0;    %r.p.m.    %output signal of the speed transducer
    Ni=10;    % V    reference speed
    N=0;    %r.p.m.    real speed
    Ii=0;    %A    reference current -initial value
    t=0;    %sec    % initial time

```

```

    tf=1;    %sec    %final time
    i=1;    %counter
%%%%%%%%%%%%%%%%%%%%%%%%%%%%%%%%%%%%%%%%%%%%%%%%%%%%%%%%%%%%%%%%%%%%%%%%
%power balance estimation
%%%%%%%%%%%%%%%%%%%%%%%%%%%%%%%%%%%%%%%%%%%%%%%%%%%%%%%%%%%%%%%%%%%%%%%%
    swcu=0;    %estimation of the copper losses
    swl=0;    %estimation of the accum. energy in the rotor inductance
    swj=0;    %estimation of the accum. energy in the motion masses
    wpr=0;    %estimation of the input energy
    wp=0;
%%%%%%%%%%%%%%%%%%%%%%%%%%%%%%%%%%%%%%%%%%%%%%%%%%%%%%%%%%%%%%%%%%%%%%%%
%Load torque estimator
%%%%%%%%%%%%%%%%%%%%%%%%%%%%%%%%%%%%%%%%%%%%%%%%%%%%%%%%%%%%%%%%%%%%%%%%
T0=0.0024    %2* T;
zita=0.707;
Mre=0;    vt2=0;    vt4=0;
taue=2* zita* T0;
k2e=2* zita/kj/T0;
while (t<=tf) ,
    vtnf(i)=Nf;    %speed vector
    vtnr(i)=Nr;    vtii(i)=Ii;
    vtn(i)=N;    vtir(i)=Ir;
    vtif(i)=If;    vtu(i)=U;
    vtia(i)=Ia;    mre(i)=Mre;
    % perturbation load torque wp
    mre(i)=Mre;
    mp(i)=wp;
    epsilon(i)=wp^2-Mre^2;
    %output signal of the speed filter at the current step (k)
    Nfu=exp(-T/Tt)*Nf+(1-exp(-T/Tt))*Ni;
    % speed feedback at the current step (k)
    Nru=exp(-T/Tt)*Nr+kt*(1-exp(-T/Tt))*N;
    %output signal of the speed controller=reference of the rotor current (k)
    Iiu=Ii+k2* tau2* (Nfu-Nru)+k2* (T-tau2)* (Nf-Nr);
    % allowable limits of the rotor current
    if Iiu>10,
        Iiu=10;
    elseif Iiu<-10,
        Iiu=-10;
    else
        Iiu=Iiu;
    end
    % filtered reference of the rotor current, at the current step (k)
    Ifu=exp(-T/Ti)*If+(1-exp(-T/Ti))*Ii;

```

```

%feedback rotor current (k)
Iru=exp(-T/Ti)*Ir+ki*(1-exp(-T/Ti))*Ia;
% output of the current controller= rotor voltage (k)
Uu=U+k1*kd*taul*(Ifu-Iru)+k1*kd*(T-taul)*(If-Ir);
%load torque estimator
vt2u=vt2+T*kj*(Cm*Ia-Mre-vt4);
Mreu=Mre+T*k2e*(vt2-N)/taue;
%rotor current (k)
Iau=exp(-T/Ta)*Ia+ka*(1-exp(-T/Ta))*(U-Ce*N);
wl(i)=La*Iau*(Iau-Ia); %acum. en. in the L.rotor inductance.at the
current sampling
swl=swl+wl(i); % acum.en. in the L.rotor through the starting
period
%rotor speed(k)
Nu=N+kj*T*(Cm*Ia-wp);
vt4u=(vt2u-Nu)*k2e;
%load torque variation
if t<=0.5,
    wp=0.5*Mr;
elseif (t<=0.6) & (t>0.5),
    wp=0.3*Mr;
elseif (t<=0.7) & (t>0.6),
    wp=0.8*Mr;
elseif (t<=0.8) & (t>0.7),
    wp=1*Mr; %alfa*t;
elseif (t<=0.9) & (t>0.8),
    wp=1*Mr;
else
    wp=1*Mr;
end
% acum. en.in the rotational mass
wj(i)=(k^2)*Jt*Nu*(Nu-N);
swj=swj+wj(i);
%energy estimation
pcu(i)=Ra*(vtia(i)^2); % copper power losses
swcut(i)=pcu(i)*T; % energy losses at each sampling time
swcu=swcu+swcut(i); % rotor energy losses
pr(i)=vtu(i)*vtia(i); % the input electrical power
wpr=wpr+pr(i)*T; % the input energy
Nf=Nfu; Nr=Nru; Ii=Iiu;
N=Nu;
Ir=Iru; %Ir(k-1)
If=Ifu; %If(k-1)
U=Uu; %U(k-1)

```

```

    Ia=Iau;      %Ia(k-1)
    Mre=Mreu;   vt2=vt2u;   vt4=vt4u;
    t=t+T;     % simulation time increment
    i=i+1;     % counter increment
end
wu=wpr-swcu-sw1-swj % DC motor output poweren.
eta=wu/wpr; %the efficiency of the DC drive
figure(1)
t=0:T:tf;
plot(vtia*Cm,vtn,'b','LineWidth',3)
title('electromechanical characteristic','FontSize',12)
xlabel('electromagnetic torque[ Nm] ','FontSize',12)
ylabel('speed[ rot/min] ','FontSize',12)
grid

fprintf('vizualizati caracteristica mecanica')
figure(2)
%t=0:T:tf-T;
t=0:T:tf;
subplot(2,2,1);
%plot(t,vtnf(1:length(t)),'c','LineWidth',3)
plot(t,vtnf,'b','LineWidth',3)
title('nfilter=f(t) ','FontSize',12)
xlabel('time[ sec] ','FontSize',12)
ylabel('Nf[ r.p.m.] ','FontSize',12)
grid

subplot(2,2,2);
plot(t,vtnr,'y','LineWidth',3)
title('Nfbck=f(t) ','FontSize',12)
xlabel('time[ sec] ','FontSize',12)
ylabel('Nfbck[ r.p.m.] ','FontSize',12)
grid

subplot(2,2,3);
plot(t,vtii,'r','LineWidth',3)
title('ref. rotor current','FontSize',12)
xlabel('time[ sec] ','FontSize',12)
ylabel('Ia* [ A] ','FontSize',12)
grid

subplot(2,2,4);

```

```
plot(t,vtif,'k','LineWidth',3)
title('Ifilter=f(t)','FontSize',12)
xlabel('time[ sec] ','FontSize',12)
ylabel('filtered Ia*[ A] ','FontSize',12)
grid
```

```
figure(3)
subplot(2,2,1);
plot(t,vtu,'b','LineWidth',3)
title('Rotor Voltage','FontSize',12)
xlabel('time[ sec] ','FontSize',12)
ylabel('Ua[ V] ','FontSize',12)
grid
```

```
subplot(2,2,2);
plot(t,vtia,'y','LineWidth',3)
title('Ia=f(t)','FontSize',12)
xlabel('time[ sec] ','FontSize',12)
ylabel('Ia[ A] ','FontSize',12)
grid
```

```
subplot(2,2,3);
plot(t,vtn,'r','LineWidth',3)
title('n=f(t)','FontSize',12)
xlabel('time[ sec] ','FontSize',12)
ylabel('speed[ r.p.m.] ','FontSize',12)
grid
```

```
subplot(2,2,4);
plot(t,mp,'r',t,mre,'k','LineWidth',3)
title('TL=f(t),TLe=f(t)','FontSize',12)
xlabel('time[ sec] ','FontSize',12)
ylabel('TL, TLe[ N*m] ','FontSize',12)
grid
fprintf('vizualizati fig.2')
```

```
figure(4)
t=0:T:tf;
%subplot(1,2,1);
plot(t,mp,'r',t,mre,'k','LineWidth',3)
title('TL=f(t),TLe=f(t)','FontSize',12)
xlabel('time[ sec] ','FontSize',12)
ylabel('TL, TLe[ N*m] ','FontSize',12)
grid
```

```

fprintf('vizualizati fig.3')
figure(5)
t=0:T:34*T;
i=1:35;
subplot(1,2,1);
plot(t,mp(i),'r','LineWidth',3)
title('Mr =f(t)', 'FontSize',12)
xlabel('time[ sec] ', 'FontSize',12)
ylabel('Mr[ N*m] ', 'FontSize',12)
grid

subplot(1,2,2);
plot(t,mre(i),'g','LineWidth',3)
title('Mr^ =f(t)', 'FontSize',12)
xlabel('time[ sec] ', 'FontSize',12)
ylabel('Mre[ N*m] ', 'FontSize',12)
grid
fprintf('vizualizati fig.4')
%energy components
swcu %copper losses
wpr %input energy
swl %accum. Energy in rotor inductance Lrotor
swj %accum. Energy in rotational mass
eta %efficiency during starting
omn=1/T0
tr=-log(0.05*sqrt(1-zita^2))/zita/omn

```

Author details

Marian Gaiceanu

Address all correspondence to: marian.gaiceanu@ieee.org

Integrated Energy Conversion Systems and Advanced Control of Complex Processes Research Center, Dunarea de Jos University of Galati, Romania

References

- [1] Gaiceanu M, Solea R, Codres B, Eni C. On-line Identification of the DC Motor Parameters by using Least Mean Square Recursive Method. Resita: Analele Universitatii "Eftimie Murgu". 2014. 1453–7397. 2(ANUL XXI):ISSN.

- [2] Rosu E, Bivol I, Nichita C, Gaiceanu M. Energetical Optimization of the Electromechanical Conversion Systems (Optimizarea energetica a sistemelor de conversie electromecanice). Bucharest: Technical House. 1999. 210 p. ISBN 973-31-1329-8.
- [3] Puangdownreonga D, Nawikavatan A, Thammarat C. Optimal design of I-PD controller for DC motor speed control system by Cuckoo Search. *Procedia Computer*. 2016;**86**:1877–0509/83–86. DOI: 10.1016/j.procs.2016.05.021.
- [4] Grignon D, Chen X, Tan Y, Qian H, Kar N. Robust load disturbance torque estimation for a DC motor drive system. *IFAC Proceedings Volumes*. 2012;**45**(13):460–466. DOI: 10.3182/20120620-3-DK-2025.00139.
- [5] Babaei M, Asgharei R, Ahmarinejad A. Electromagnetic torque and speed estimators for permanent magnet synchronous motor drive systems. *Energy Procedia*. 2016;**100**:291–296. DOI: 10.1016/j.egypro.2016.10.180.
- [6] Thanga Raj C, Srivastava SP, Agarwal P. Differential evolution based optimal control of induction motor serving to textile industry. *IAENG International Journal of Computer Science*. 2008;**35**(2):IJCS_35_2_03.
- [7] Gaiceanu M. Linear quadratic regulator for the three-phase grid connected power converter. In: 2nd International Conference on Micro Nano Devices, Structure and Computing Systems; January 23–24; Shenzhen, China. 2013.
- [8] Carnegie Mellon University. Control Tutorials for MATLAB and Simulink [Internet]. 2006. Available from: <http://ctms.engin.umich.edu> [Accessed: 2016].
- [9] Springer International Publishing AG, Switzerland

IntechOpen

